

## Suppression of Metal-to-Semiconductor Transition in Nanocrystalline $\text{Ti}_4\text{O}_7$ via Crystallite Size Control

Tomoko Kubota,<sup>a</sup> Riku Seiki,<sup>a</sup> Takahiro Kondo,<sup>a,b</sup> Verdad C. Agulto,<sup>c</sup> Makoto Nakajima,<sup>c</sup>  
Shin-ichi Ohkoshi,<sup>d</sup> and Hiroko Tokoro<sup>\*a,d</sup>

<sup>a</sup> *Department of Materials Science, Institute of Pure and Applied Sciences, University of Tsukuba,  
1-1-1 Tennodai, Tsukuba, Ibaraki 305-8573, Japan*

<sup>b</sup> *Tsukuba Institute for Advanced Research (TIAR), University of Tsukuba,  
1-1-1 Tennodai, Tsukuba, Ibaraki 305-8573, Japan*

<sup>c</sup> *Institute of Laser Engineering, The University of Osaka,  
2-6 Yamadaoka, Suita, Osaka 565-0871, Japan*

<sup>d</sup> *Department of Chemistry, School of Science, The University of Tokyo,  
7-3-1 Hongo, Bunkyo-ku, Tokyo 113-0033, Japan*

	Contents	Page
§ 1.	Crystallographic data ..... Tables S1–S4	S2–S10
§ 2.	Size distribution ..... Figure S1	S11
§ 3.	TEM images ..... Figure S2	S12
§ 4.	XPS spectra at room temperature ..... Figures S3, S4	S13
§ 5.	THz conductivity spectrum ..... Figure S5	S14
§ 6.	Temperature dependence of Gibbs free energy ..... Figure S6	S15
§ 7.	Gaussian distribution of crystallite size ..... Figure S7	S16
§ 8.	Relationship between Gibbs free energy, crystallite size, and transition enthalpy ..... S17	S17

## § 1. Crystallographic data.

**Table S1.** Crystallographic data of **1**.  $R_{wp}$ ,  $S$ , and  $\chi^2$  values were 4.64%, 3.24, and 10.5, respectively.

Crystal system	Triclinic	Atoms	$x$	$y$	$Z$
Space group	$P\bar{1}$	Ti(1)	0.240(3)	0.160(2)	0.075(1)
$a$ (Å)	5.5980(5)	Ti(2)	0.189(2)	0.646(2)	0.037(9)
$b$ (Å)	7.1294(5)	Ti(3)	0.236(3)	0.639(3)	0.567(1)
$c$ (Å)	12.4514(10)	Ti(4)	0.231(3)	0.150(2)	0.576(1)
$\alpha$ (°)	95.070(6)	Ti(5)	0.655(4)	0.448(3)	0.204(1)
$\beta$ (°)	95.068(5)	Ti(6)	0.696(3)	0.937(2)	0.212(1)
$\gamma$ (°)	108.837(4)	Ti(7)	0.672(4)	0.938(3)	0.695(1)
$V$ (Å <sup>3</sup> )	464.87(6)	Ti(8)	0.671(3)	0.436(2)	0.713(1)
Quantitative value (%)	100	O(1)	0.089(9)	0.870(6)	0.020(3)
Crystallite size (nm)	11.11(17)	O(2)	0.594(9)	0.800(8)	0.042(4)
		O(3)	0.813(9)	0.495(6)	0.104(3)
		O(4)	0.504(8)	0.189(6)	0.217(3)
		O(5)	0.024(9)	0.079(7)	0.199(3)
		O(6)	0.274(8)	0.769(7)	0.210(3)
		O(7)	0.254(8)	0.273(7)	0.747(3)
		O(8)	0.023(10)	0.549(7)	0.697(3)
		O(9)	0.524(8)	0.648(7)	0.647(3)
		O(10)	0.229(7)	0.871(6)	0.639(3)
		O(11)	0.848(9)	0.957(7)	0.589(3)
		O(12)	0.592(9)	0.276(7)	0.559(3)
		O(13)	0.060(8)	0.348(6)	0.561(3)
		O(14)	0.318(6)	0.412(6)	0.117(3)

**Table S2.** Miller indices (hkl) corresponding to different diffraction peaks are listed. The  $2\theta$  values were determined by Rietveld refinement for **1**.

$2\theta$ (degree)	$h$	$k$	$l$	$2\theta$ (degree)	$h$	$k$	$l$	$2\theta$ (degree)	$h$	$k$	$l$	$2\theta$ (degree)	$h$	$k$	$l$	$2\theta$ (degree)	$h$	$k$	$l$
14.243	0	1	-1	33.952	2	0	-1	41.335	2	1	-2	49.077	0	2	-6	53.738	3	-2	-3
14.380	0	0	2	34.084	2	0	0	41.391	1	1	4	49.124	3	-1	0	53.890	1	3	2
15.824	0	1	1	34.266	2	-1	-2	41.619	2	-2	-3	49.418	1	3	-2	54.045	1	3	-4
16.853	1	0	0	34.534	1	-1	4	42.007	0	3	1	49.506	2	-3	-3	54.250	2	-4	0
17.487	1	0	-1	35.137	1	-2	-3	42.061	1	-3	-2	49.595	2	1	3	54.264	3	0	-3
17.628	1	-1	0	35.379	1	1	-4	42.259	0	2	4	49.630	1	0	6	54.357	0	4	-1
18.315	0	1	-2	35.399	2	0	-2	42.320	2	0	-4	49.961	3	-1	-2	54.411	1	-4	3
18.881	1	-1	-1	35.562	1	0	4	42.402	1	0	5	50.030	3	-2	0	54.436	2	-4	1
19.151	1	0	1	35.592	1	1	3	42.587	2	1	1	50.470	3	-1	1	54.458	1	1	-7
19.226	1	-1	1	35.692	2	-2	0	42.627	2	-2	3	50.499	1	-3	-4	54.503	2	1	4
20.767	0	1	2	35.899	1	2	-1	42.765	1	-3	3	50.656	1	2	4	54.733	3	-3	0
20.796	1	0	-2	36.264	2	-2	-1	42.773	0	2	-5	50.682	2	2	-2	54.740	1	1	6
21.642	0	0	3	36.277	1	2	0	43.303	1	2	-4	50.774	2	2	0	54.813	0	4	0
22.530	1	-1	-2	36.468	0	0	5	43.667	0	3	-3	50.974	1	-2	6	54.820	1	-1	-7
23.111	1	-1	2	36.643	2	-2	1	44.107	0	0	6	51.087	1	3	1	55.002	0	4	-2
23.566	1	0	2	37.034	1	2	-2	44.518	0	1	-6	51.096	3	-2	1	55.075	3	-3	-1
23.969	0	1	-3	37.120	0	2	-4	45.375	1	0	-6	51.194	1	3	-3	55.085	1	-4	-2
24.714	1	1	-1	37.288	0	1	-5	45.532	1	2	3	51.230	2	-2	-5	55.097	2	2	-4
24.757	1	1	0	37.550	2	-1	-3	45.569	2	1	2	51.309	1	-4	1	55.165	2	-4	-1
26.355	1	-2	0	38.130	1	2	1	45.639	2	-1	4	51.355	2	1	-5	55.283	3	-1	-4
26.612	0	2	0	38.176	1	-3	0	45.995	2	-2	-4	51.454	2	-1	5	55.309	0	2	6
26.698	0	2	-1	38.270	2	0	-3	46.359	2	-3	-2	51.719	0	3	-5	55.487	3	-3	1
26.741	1	1	-2	38.300	2	-2	-2	46.585	1	-2	-5	51.732	3	0	-1	55.620	0	1	7
26.838	0	1	3	38.330	1	-3	1	46.725	1	-3	4	52.064	0	1	-7	55.716	2	-4	2
27.687	1	-1	-3	38.366	1	0	-5	47.213	0	3	-4	52.158	3	0	0	55.779	1	-1	7
28.406	1	-1	3	38.636	1	-2	4	47.235	2	-2	4	52.311	1	-4	2	56.304	3	0	2
28.712	0	2	-2	38.864	2	0	2	47.266	2	-1	-5	52.357	2	2	-3	56.385	3	-1	3
28.992	0	0	4	39.022	2	-2	2	47.310	2	0	-5	52.445	3	0	-2	56.474	3	-2	3
29.205	1	0	3	39.457	1	-3	-1	47.392	1	-1	-6	52.661	2	-2	5	56.499	3	-3	-2
29.550	1	-2	2	40.346	1	-1	-5	47.547	1	1	-6	52.712	2	-3	4	56.512	1	2	5
30.400	0	1	-4	40.390	2	1	-1	47.811	1	1	5	52.728	1	-4	-1	56.722	0	4	-3
30.735	1	-2	-2	40.391	0	3	0	47.927	0	1	6	52.924	3	-1	2	57.037	0	3	-6
31.790	1	0	-4	40.504	1	-2	-4	48.013	1	2	-5	53.059	2	0	-6	57.100	3	-2	-4
31.960	0	2	2	40.552	0	1	5	48.210	2	0	4	53.236	1	-2	-6	57.118	3	0	-4
32.148	2	-1	0	40.575	2	-1	3	48.304	1	-1	6	53.273	3	-2	2	57.144	2	-4	-2
32.323	0	2	-3	40.819	2	1	0	48.512	0	2	5	53.274	2	-1	-6	57.235	1	-3	6
32.393	2	-1	-1	41.150	1	1	-5	48.773	2	-3	3	53.521	1	2	-6	57.524	2	-3	5
33.500	0	1	4	41.208	1	-1	5	48.781	0	3	3	53.603	0	3	4	57.528	1	-4	4
33.561	2	-1	1	41.255	0	3	-2	48.796	1	3	-1	53.635	2	-3	-4	57.664	1	3	3
33.731	1	-1	-4	41.288	1	2	2	48.952	3	-1	-1	53.703	3	0	1	57.862	1	3	-5

$2\theta$ (degree)	$h$	$k$	$l$	$2\theta$ (degree)	$h$	$k$	$l$	$2\theta$ (degree)	$h$	$k$	$l$	$2\theta$ (degree)	$h$	$k$	$l$	$2\theta$ (degree)	$h$	$k$	$l$
57.897	2	-1	6	63.017	3	1	2	66.935	2	-5	1	70.473	1	-3	8	74.801	2	-1	-9
57.964	1	-2	7	63.063	0	3	-7	66.994	2	-5	0	70.522	2	-4	6	74.825	4	-1	3
58.040	2	-4	3	63.127	0	4	-5	67.048	4	-2	-1	70.636	3	-4	-4	74.848	2	2	-8
58.613	2	-3	-5	63.196	3	-4	-1	67.250	4	-2	0	70.685	3	2	-4	74.903	3	-4	-5
58.696	3	1	0	63.252	0	2	-8	67.421	2	3	2	70.754	2	-3	-7	75.288	2	0	8
58.774	2	-2	6	63.267	1	4	-2	67.476	3	2	-2	70.802	4	-3	1	75.361	2	2	6
58.803	2	2	-5	63.377	2	2	-6	67.631	2	0	7	70.861	4	-3	-2	75.508	2	3	4
58.917	0	4	2	63.541	1	-3	7	67.655	0	4	-6	70.884	1	-1	-9	75.558	3	0	6
59.133	2	2	3	63.634	2	3	-3	67.730	1	3	5	71.022	3	1	4	75.587	4	-3	-4
59.193	0	3	5	63.646	1	-1	8	67.818	4	-2	-2	71.038	2	3	3	75.598	3	-5	-2
59.449	2	0	-7	63.665	0	1	8	67.864	1	-5	3	71.261	3	-2	6	75.601	4	-4	0
59.456	0	4	-4	63.679	1	4	0	67.897	4	-1	0	71.603	4	-1	2	75.738	4	-2	-5
59.707	1	2	-7	63.759	2	-2	-7	68.018	1	4	2	71.768	4	0	0	75.816	4	0	2
59.872	3	0	3	63.773	2	2	4	68.020	4	-1	-2	71.811	0	5	1	75.831	4	-4	-1
59.941	3	1	-3	63.879	3	-3	4	68.036	1	-2	-8	72.080	1	-4	7	75.961	1	4	4
59.942	0	1	-8	64.013	2	-4	-4	68.117	3	2	0	72.197	4	-2	-4	76.097	2	4	-1
60.084	0	0	8	64.315	3	0	4	68.480	3	-3	5	72.380	0	3	7	76.100	2	4	-2
60.168	2	1	5	64.336	3	-1	-6	68.556	0	0	9	72.479	2	-1	8	76.179	2	-5	5
60.364	3	1	1	64.339	2	-3	-6	68.672	1	0	-9	72.506	2	-5	4	76.215	1	-2	-9
60.389	1	-2	-7	64.702	2	3	1	68.955	1	-3	-7	72.561	3	2	2	76.264	3	1	5
60.509	1	0	-8	64.734	3	-4	-2	69.075	2	1	-8	72.673	4	-3	2	76.296	4	-4	1
60.560	2	0	6	65.210	1	0	8	69.197	2	2	5	72.734	1	-5	-3	76.302	2	-4	7
60.747	3	-1	4	65.374	1	4	1	69.282	4	-1	1	72.769	4	-3	-3	76.308	2	1	-9
60.915	3	0	-5	65.445	1	-2	8	69.378	2	-3	7	72.832	2	-2	8	76.330	2	-3	8
61.334	2	-4	4	65.465	0	3	6	69.526	4	-1	-3	72.901	2	-5	-3	76.467	3	-1	-8
61.366	3	-2	-5	65.504	2	-2	7	69.544	4	-2	-3	72.982	0	4	-7	76.611	0	5	-5
61.565	1	-4	5	65.518	2	-4	5	69.638	0	5	-1	73.234	3	-5	0	76.678	2	-5	-4
61.838	1	1	-8	65.548	3	-2	5	69.699	1	1	-9	73.451	3	-5	1	76.782	1	-5	-4
62.139	1	1	7	65.619	1	-5	1	69.717	2	-5	3	73.496	2	1	7	76.934	0	1	-10
62.154	1	-3	-6	65.789	3	1	-5	69.741	0	3	-8	73.645	1	0	9	76.985	4	-4	-2
62.158	2	3	-1	65.849	2	3	-4	69.868	4	-3	0	73.673	3	2	-5	77.016	2	4	0
62.364	3	-3	-4	65.916	3	-1	5	69.888	4	-3	-1	73.875	3	-3	6	77.323	1	0	-10
62.393	2	3	-2	65.964	1	-5	0	70.004	2	-5	-2	73.888	1	3	6	77.480	0	0	10
62.398	3	1	-4	66.425	2	0	-8	70.019	1	1	8	73.983	2	0	-9	77.537	3	2	-6
62.432	0	4	3	66.437	1	-4	6	70.039	3	-1	-7	74.055	1	4	-6	77.707	3	-2	7
62.489	2	1	-7	66.447	3	-2	-6	70.049	3	1	-6	74.193	1	3	-8	77.811	1	2	8
62.602	0	2	7	66.505	1	2	-8	70.252	0	5	0	74.268	2	-4	-6	77.850	4	1	-1
62.636	1	-1	-8	66.509	2	1	6	70.329	3	-4	4	74.290	0	5	2	77.862	2	3	-7
62.651	3	-4	0	66.817	0	4	4	70.395	0	2	8	74.529	3	-4	5	77.908	4	-4	2
63.007	1	2	6	66.821	1	4	-4	70.408	1	-5	4	74.600	3	-5	2	77.948	4	1	-2

$2\theta$ (degree)	$h$	$k$	$l$	$2\theta$ (degree)	$h$	$k$	$l$	$2\theta$ (degree)	$h$	$k$	$l$	$2\theta$ (degree)	$h$	$k$	$l$	$2\theta$ (degree)	$h$	$k$	$l$
77.972	0	4	6	81.691	2	2	-9	85.448	0	5	-7	88.358	4	-5	3	91.735	2	-6	-4
77.978	4	0	-5	81.695	2	-6	0	85.609	1	-4	9	88.418	1	3	8	91.742	5	-3	2
78.037	1	-3	9	81.898	1	-6	2	85.655	2	-3	-9	88.445	4	2	0	91.747	3	-3	-9
78.150	3	-5	-3	81.917	3	3	1	85.841	4	-4	-5	88.521	4	0	5	91.867	1	5	4
78.439	1	1	9	81.930	4	0	-6	85.854	3	-1	8	88.562	0	2	-11	91.884	3	0	-10
78.470	3	-1	7	81.944	1	2	-10	86.010	4	-5	-2	88.563	5	-3	0	91.978	4	1	-7
78.729	2	-2	-9	82.005	4	-4	-4	86.070	2	-6	4	88.646	5	-1	-1	92.073	5	-1	-4
78.742	0	2	9	82.022	1	-2	10	86.075	2	-5	7	88.759	5	-2	1	92.267	0	4	8
78.852	3	-2	-8	82.042	1	-6	0	86.091	4	-5	2	88.794	1	3	-10	92.294	2	-1	-11
78.865	2	4	-4	82.215	4	-2	5	86.174	3	-2	-9	88.975	5	-3	-2	92.308	2	-5	8
79.076	0	4	-8	82.251	3	2	-7	86.263	0	1	-11	88.989	3	-6	-2	92.340	1	0	11
79.079	3	3	-1	82.298	3	1	6	86.294	1	-3	10	89.144	3	1	7	92.400	0	6	-5
79.116	4	-3	4	82.634	1	0	10	86.299	3	-6	0	89.272	1	-5	8	92.409	1	-6	6
79.285	4	-3	-5	82.847	2	-4	8	86.301	3	-6	1	89.314	2	2	-10	92.430	2	-3	10
79.489	0	2	-10	82.862	2	-6	-1	86.531	4	1	3	89.405	2	-6	5	92.688	3	-4	-8
79.559	3	-4	6	83.021	4	1	2	86.665	0	6	-2	89.468	2	-2	10	92.748	5	-4	0
79.631	3	-5	4	83.171	2	-1	-10	86.911	2	3	6	89.542	2	-1	10	92.755	2	5	-3
79.651	1	-1	-10	83.183	1	-6	3	86.964	5	-2	-1	89.591	0	6	-4	92.911	3	-2	9
79.662	1	5	-3	83.289	1	-5	7	86.985	0	5	5	89.640	4	-1	6	92.949	0	5	6
80.040	3	-3	7	83.422	4	0	4	86.989	3	-3	8	89.679	2	4	4	92.978	5	-3	-4
80.137	4	-2	-6	83.471	3	-5	5	87.137	1	1	-11	89.715	2	4	-7	93.116	2	-5	-7
80.147	1	-4	-7	83.471	1	-6	-1	87.195	3	-6	-1	89.803	4	2	-4	93.125	1	-6	-4
80.397	4	1	1	83.532	2	3	-8	87.203	3	-6	2	89.844	3	0	8	93.153	4	2	2
80.422	4	-4	3	83.821	4	-4	4	87.214	2	-2	-10	89.951	2	2	8	93.300	5	-1	2
80.560	3	2	4	83.841	4	-3	-6	87.239	1	4	6	90.033	5	-1	-3	93.364	5	0	-1
80.602	0	5	-6	83.851	4	-1	5	87.328	4	2	-2	90.037	2	3	-9	93.375	1	-3	-10
80.656	2	-1	9	83.985	2	-3	9	87.393	4	1	-6	90.197	2	-4	9	93.403	5	0	-2
80.706	2	-5	6	84.227	2	1	-10	87.401	1	-5	-6	90.314	1	-1	11	93.571	5	-4	-2
80.770	1	3	7	84.249	4	-5	0	87.438	1	5	3	90.527	5	-3	-3	93.583	1	-4	10
80.794	1	-1	10	84.278	3	-3	-8	87.484	1	-4	-8	90.555	4	-4	-6	93.636	2	-6	6
80.799	2	3	5	84.308	3	3	-5	87.509	1	1	10	90.777	0	1	11	93.659	0	4	-10
80.882	4	1	-4	84.315	1	5	-5	87.625	2	-4	-8	90.850	5	-1	1	93.776	3	-5	7
81.109	1	3	-9	84.654	1	4	-8	87.750	0	2	10	90.925	4	1	4	93.809	3	4	-3
81.112	0	1	10	84.682	3	3	2	87.811	4	-2	6	91.003	5	-2	2	93.888	2	3	7
81.147	2	1	8	84.720	4	-5	1	87.811	3	2	-8	91.007	5	-2	-4	94.003	1	-5	-7
81.241	1	5	1	84.900	3	-2	8	87.974	1	5	-6	91.074	3	-5	-6	94.284	4	-2	7
81.433	2	-6	1	84.928	2	-6	-2	88.097	4	-4	5	91.358	4	-5	-4	94.334	3	-2	-10
81.516	1	-6	1	85.079	0	3	-10	88.117	4	2	-3	91.481	4	-2	-8	94.508	4	0	6
81.578	2	4	2	85.367	1	-6	4	88.247	0	3	9	91.589	0	6	2	94.586	3	4	0
81.673	1	-5	-5	85.409	3	-4	7	88.332	3	3	3	91.697	3	-6	4	94.682	5	-3	3

$2\theta$ (degree)	$h$	$k$	$l$	$2\theta$ (degree)	$h$	$k$	$l$
94.794	3	-3	9	97.991	4	-6	-2
95.068	2	4	5	98.209	5	-2	4
95.069	0	6	3	98.216	5	-2	-6
95.110	2	4	-8	98.275	5	-4	3
95.221	3	1	-10	98.456	2	-4	10
95.274	3	-6	-4	98.504	0	2	-12
95.289	4	-3	7	98.544	2	2	9
95.351	3	4	-4	98.794	2	-6	7
95.364	2	5	1	98.828	2	1	10
95.374	1	-3	11	98.879	5	-1	-6
95.409	1	2	10	98.881	2	-7	2
95.524	5	-4	2	98.941	5	0	-5
95.561	2	-4	-9	99.032	3	2	7
95.566	4	-3	-8	99.042	2	-2	11
95.587	4	-5	5	99.324	2	-1	11
95.810	4	-6	0	99.325	4	-6	3
95.987	5	0	1	99.382	1	-1	-12
96.075	4	-6	1	99.476	2	-5	9
96.117	0	6	-6	99.478	0	6	4
96.149	1	-5	9	99.630	3	4	2
96.227	4	1	5	99.703	4	3	-2
96.344	1	6	-2	99.749	3	-4	9
96.395	0	1	-12	99.830	1	-7	1
96.495	2	-6	-5	99.856	0	5	7
96.659	5	-1	3				
96.664	1	0	-12				
96.868	4	2	3				
96.940	1	3	9				
97.101	1	6	-3				
97.168	3	-5	-7				
97.211	1	5	5				
97.245	4	-6	2				
97.345	0	0	12				
97.362	1	3	-11				
97.410	0	3	10				
97.421	1	1	11				
97.446	2	3	-10				
97.479	4	1	-8				
97.541	1	6	0				
97.786	0	5	-9				

**Table S3.** Crystallographic data of **2**.  $R_{wp}$ ,  $S$ , and  $\chi^2$  values were 4.20%, 2.87, and 8.26, respectively.

Crystal system	Triclinic	Atoms	$x$	$y$	$z$
Space group	$P\bar{1}$	Ti(1)	0.234(2)	0.154(2)	0.0775(10)
$a$ (Å)	5.5983(2)	Ti(2)	0.219(3)	0.651(2)	0.0671(11)
$b$ (Å)	7.1241(2)	Ti(3)	0.221(2)	0.6482(18)	0.5504(10)
$c$ (Å)	12.4606(3)	Ti(4)	0.213(3)	0.162(2)	0.5651(11)
$\alpha$ (°)	95.057(2)	Ti(5)	0.673(3)	0.435(2)	0.2046(10)
$\beta$ (°)	95.147(2)	Ti(6)	0.684(3)	0.939(3)	0.2017(10)
$\gamma$ (°)	108.777(2)	Ti(7)	0.672(3)	0.938(2)	0.6981(9)
$V$ (Å <sup>3</sup> )	465.00(2)	Ti(8)	0.699(3)	0.444(2)	0.7043(10)
Quantitative value (%)	100	O(1)	0.090(9)	0.855(6)	0.018(3)
Crystallite size (nm)	29.6(4)	O(2)	0.587(9)	0.787(7)	0.053(3)
		O(3)	0.863(9)	0.491(6)	0.082(3)
		O(4)	0.522(8)	0.140(6)	0.154(3)
		O(5)	0.035(9)	0.068(7)	0.193(3)
		O(6)	0.278(9)	0.769(6)	0.232(2)
		O(7)	0.286(9)	0.282(7)	0.718(3)
		O(8)	0.027(9)	0.569(7)	0.704(3)
		O(9)	0.523(8)	0.646(6)	0.676(2)
		O(10)	0.329(10)	0.920(8)	0.636(3)
		O(11)	0.850(9)	1.008(6)	0.585(3)
		O(12)	0.591(9)	0.280(7)	0.557(3)
		O(13)	0.105(8)	0.368(6)	0.521(3)
		O(14)	0.312(9)	0.421(7)	0.133(3)

**Table S4.** Miller indices (hkl) corresponding to different diffraction peaks are listed. The  $2\theta$  values were determined by Rietveld refinement for **2**.

$2\theta$ (degree)	$h$	$k$	$l$	$2\theta$ (degree)	$h$	$k$	$l$	$2\theta$ (degree)	$h$	$k$	$l$	$2\theta$ (degree)	$h$	$k$	$l$	$2\theta$ (degree)	$h$	$k$	$l$
13.218	0	1	0	34.538	1	-1	4	42.281	2	0	-4	50.035	3	-2	0	55.335	2	2	2
14.244	0	1	-1	35.130	1	-2	-3	42.395	1	0	5	50.467	3	-1	1	55.512	3	-3	1
14.373	0	0	2	35.351	1	1	-4	42.648	2	-2	3	50.643	1	2	4	55.754	2	-4	2
16.846	1	0	0	35.373	2	0	-2	42.766	0	2	-5	50.649	2	2	-2	55.773	1	-1	7
17.474	1	0	-1	35.558	1	0	4	42.787	1	-3	3	50.749	2	2	0	55.901	0	2	-7
17.634	1	-1	0	35.584	1	1	3	43.081	2	0	3	50.980	1	-2	6	55.970	1	-3	-5
18.313	0	1	-2	35.704	2	-2	0	43.279	1	2	-4	51.203	2	-2	-5	56.292	3	0	2
18.879	1	-1	-1	36.265	1	2	0	43.579	2	-3	0	51.307	2	1	-5	56.390	3	-1	3
19.148	1	0	1	36.269	2	-2	-1	43.671	0	3	-3	51.373	3	-2	-2	56.497	1	2	5
20.762	0	1	2	36.451	0	0	5	44.087	0	0	6	51.461	2	-1	5	56.508	2	1	-6
20.778	1	0	-2	36.469	2	-1	2	44.099	2	-3	1	51.473	1	-4	0	56.729	0	4	-3
21.632	0	0	3	36.660	2	-2	1	44.352	2	-3	-1	52.070	3	-1	-3	57.068	3	0	-4
22.521	1	-1	-2	36.663	0	2	3	44.501	0	1	-6	52.136	3	0	0	57.072	3	-2	-4
23.565	1	0	2	37.017	1	2	-2	44.511	1	-2	5	52.338	1	-4	2	57.145	2	-2	-6
23.964	0	1	-3	37.116	0	2	-4	45.339	1	0	-6	52.409	3	0	-2	57.212	1	0	7
24.699	1	1	-1	37.526	2	-1	-3	45.520	1	2	3	52.680	2	-2	5	57.249	1	-3	6
24.745	1	1	0	38.195	1	-3	0	45.555	2	1	2	52.716	1	0	-7	57.336	3	-3	2
26.369	1	-2	0	38.297	2	-2	-2	45.647	2	-1	4	52.745	1	-4	-1	57.554	1	-4	4
26.615	0	2	0	38.335	1	0	-5	45.876	2	-3	2	53.008	2	0	-6	57.966	1	-2	7
26.702	0	2	-1	38.649	1	-2	4	45.976	2	-2	-4	53.209	1	-2	-6	58.024	3	1	-1
26.829	0	1	3	38.859	2	0	2	46.367	2	-3	-2	53.289	3	-2	2	58.596	2	-3	-5
26.850	1	1	1	39.042	2	-2	2	46.565	1	-2	-5	53.595	0	3	4	58.754	2	2	-5
27.671	1	-1	-3	39.470	1	-3	-1	46.746	1	-3	4	53.627	2	-3	-4	58.791	2	-2	6
28.413	1	-1	3	39.550	1	2	-3	46.935	2	1	-4	53.687	3	0	1	58.919	0	4	2
28.714	0	2	-2	39.926	1	-3	2	47.215	0	3	-4	53.879	1	3	2	59.345	3	-1	-5
28.979	0	0	4	40.140	0	3	-1	47.228	2	-1	-5	54.067	2	0	5	59.462	0	4	-4
29.203	1	0	3	40.319	1	-1	-5	47.256	2	-2	4	54.281	2	-4	0	59.669	1	2	-7
29.568	1	-2	2	40.363	2	1	-1	47.265	2	0	-5	54.417	1	1	-7	59.863	3	0	3
30.390	0	1	-4	40.490	1	-2	-4	47.360	1	-1	-6	54.438	1	-4	3	59.891	3	1	-3
30.736	1	-2	-2	40.535	0	1	5	47.905	0	1	6	54.472	2	-4	1	59.915	0	1	-8
31.763	1	0	-4	40.584	2	-1	3	47.984	1	2	-5	54.492	2	1	4	60.054	0	0	8
31.958	0	2	2	40.797	2	1	0	48.207	2	0	4	54.725	1	1	6	60.156	2	1	5
32.323	0	2	-3	41.118	1	1	-5	48.496	0	2	5	54.783	1	-1	-7	60.162	3	-3	3
32.385	2	-1	-1	41.210	1	-1	5	48.784	1	3	-1	54.821	0	4	0	60.338	3	1	1
33.487	0	1	4	41.278	1	2	2	48.805	2	-3	3	55.011	0	4	-2	60.463	1	0	-8
33.571	1	-2	3	41.381	1	1	4	48.935	3	-1	-1	55.053	2	2	-4	60.556	2	0	6
33.709	1	-1	-4	41.608	2	-2	-3	49.065	0	2	-6	55.087	3	-3	-1	60.617	3	-2	4
33.932	2	0	-1	42.010	0	3	1	49.403	1	3	-2	55.098	1	-4	-2	60.753	3	-1	4
34.070	2	0	0	42.068	1	-3	-2	49.506	2	-3	-3	55.242	3	-1	-4	60.857	3	0	-5
34.249	2	-1	-2	42.248	0	2	4	49.583	2	1	3	55.289	0	2	6	61.329	3	-2	-5

$2\theta$ (degree)	$h$	$k$	$l$	$2\theta$ (degree)	$h$	$k$	$l$	$2\theta$ (degree)	$h$	$k$	$l$	$2\theta$ (degree)	$h$	$k$	$l$	$2\theta$ (degree)	$h$	$k$	$l$
61.375	2	-4	4	66.978	2	-5	1	71.596	4	-1	2	75.795	4	0	2	79.825	3	3	-3
61.793	1	1	-8	67.002	2	-1	-8	71.719	3	-3	-6	75.946	1	4	4	79.977	3	-4	-6
62.134	1	-3	-6	67.041	3	-4	3	71.736	4	0	0	76.066	2	4	-2	80.075	3	-3	7
62.430	0	4	3	67.247	4	-2	0	71.839	3	-1	6	76.104	3	2	3	80.079	4	-2	-6
62.512	1	3	-6	67.308	1	-5	-1	72.158	4	-2	-4	76.168	1	-2	-9	80.124	1	-4	-7
62.576	0	2	7	67.427	3	2	-2	72.229	3	-2	-7	76.235	2	1	-9	80.358	4	1	1
62.593	1	-1	-8	67.448	4	-1	-1	72.356	0	3	7	76.338	2	-4	7	80.653	2	-1	9
62.683	3	-4	0	67.625	2	0	7	72.480	2	-1	8	76.347	1	-3	-8	80.774	1	-1	10
62.686	1	-4	-4	67.654	0	4	-6	72.530	3	2	2	76.352	2	-3	8	80.797	2	-2	9
62.989	1	2	6	67.745	1	-4	-5	72.698	4	-3	2	76.688	2	-5	-4	81.063	1	3	-9
63.129	0	4	-5	67.798	4	-2	-2	72.756	4	-3	-3	76.788	1	-5	-4	81.069	0	1	10
63.130	2	-3	6	67.967	1	3	-7	72.843	2	-2	8	76.988	2	4	0	81.129	2	1	8
63.255	1	4	-2	67.996	1	-2	-8	72.919	2	-5	-3	76.996	4	-4	-2	81.169	1	4	5
63.323	2	2	-6	68.007	1	4	2	72.977	0	4	-7	77.265	1	0	-10	81.231	1	5	1
63.634	0	1	8	68.079	3	2	0	73.500	3	-5	1	77.439	0	0	10	81.552	2	4	2
63.636	1	-1	8	68.515	3	-3	5	73.578	4	-2	3	77.462	3	2	-6	81.617	2	2	-9
63.669	1	4	0	68.521	0	0	9	73.605	3	2	-5	77.585	3	-3	-7	81.671	1	-5	-5
63.716	2	-2	-7	68.621	1	0	-9	73.624	1	0	9	77.662	0	5	3	81.741	2	-6	0
63.754	2	2	4	68.943	2	3	-5	73.855	1	2	-9	77.728	3	-2	7	81.847	4	0	-6
64.015	2	-4	-4	69.009	2	1	-8	73.868	1	3	6	77.785	1	2	8	81.887	1	2	-10
64.279	3	-1	-6	69.270	4	-1	1	73.880	1	-5	5	77.799	4	1	-1	81.935	1	-6	2
64.309	3	0	4	69.403	2	-3	7	73.911	3	-3	6	77.803	2	3	-7	81.997	4	-4	-4
64.313	2	-3	-6	69.483	4	-1	-3	73.913	2	0	-9	77.905	4	0	-5	82.009	1	-2	10
64.546	1	4	-3	69.725	0	3	-8	73.989	3	-5	-1	77.950	4	-4	2	82.074	1	-6	0
64.678	2	3	1	69.974	3	-1	-7	74.029	1	4	-6	77.956	0	4	6	82.091	2	0	-10
64.751	3	-4	-2	69.978	3	1	-6	74.153	1	3	-8	78.037	1	1	-10	82.236	4	-2	5
65.193	1	0	8	69.997	1	1	8	74.252	2	-4	-6	78.170	3	-5	-3	82.241	2	2	7
65.443	1	-2	8	70.364	0	2	8	74.295	0	5	2	78.179	1	-5	6	82.300	3	0	7
65.446	0	3	6	70.377	3	-4	4	74.578	3	-4	5	78.412	1	1	9	82.607	1	0	10
65.501	3	0	-6	70.546	4	-2	2	74.654	3	-5	2	78.477	3	-1	7	82.881	2	-4	8
65.519	2	-2	7	70.561	2	-4	6	74.735	2	-1	-9	78.480	1	-4	8	83.096	2	-1	-10
65.558	2	-4	5	70.623	3	2	-4	74.782	2	2	-8	78.669	2	-2	-9	83.316	1	-5	7
65.569	3	-2	5	70.634	3	-4	-4	74.823	4	-1	3	78.787	3	-2	-8	83.409	4	0	4
65.924	3	-1	5	70.720	2	-3	-7	75.279	2	0	8	78.913	1	4	-7	83.534	3	-5	5
66.362	2	0	-8	70.822	4	-3	1	75.341	2	2	6	78.916	4	-1	4	83.612	4	1	-5
66.402	3	-2	-6	70.931	3	0	-7	75.485	2	3	4	79.031	3	3	-1	83.675	4	-3	5
66.459	1	-4	6	71.005	3	1	4	75.553	3	0	6	79.066	0	4	-8	83.872	4	-4	4
66.462	1	2	-8	71.064	0	2	-9	75.564	4	-3	-4	79.251	4	-3	-5	83.886	1	5	2
66.803	1	4	-4	71.283	3	-2	6	75.627	3	-5	-2	79.593	1	-1	-10	84.223	3	-3	-8
66.811	0	4	4	71.409	4	0	-2	75.629	4	-4	0	79.608	3	-4	6	84.236	3	3	-5

$2\theta$ (degree)	$h$	$k$	$l$	$2\theta$ (degree)	$h$	$k$	$l$	$2\theta$ (degree)	$h$	$k$	$l$	$2\theta$ (degree)	$h$	$k$	$l$
84.457	4	-1	-7	88.388	1	3	8	92.414	0	6	-5	96.334	4	-1	7
84.716	4	-5	-1	88.389	4	2	0	92.447	1	-6	6	96.335	1	6	-2
84.772	4	-5	1	88.480	1	-6	5	92.644	3	-4	-8	96.341	0	1	-12
84.920	3	-2	8	88.510	4	0	5	92.772	5	-4	0	96.458	2	-2	-11
84.962	2	-6	-2	88.522	0	2	-11	92.839	3	3	4	96.586	1	0	-12
85.163	2	4	3	89.030	3	-6	-2	92.935	0	5	6	96.647	5	-1	3
85.165	2	4	-6	89.200	4	-3	-7	93.107	4	2	2	96.862	3	1	8
85.309	4	-2	-7	89.230	2	2	-10	93.109	3	4	-2	97.137	4	-1	-9
85.406	1	-6	4	89.465	2	-6	5	93.137	1	-6	-4	97.147	3	-5	-7
85.619	1	-4	9	89.472	2	-2	10	93.321	1	-3	-10	97.287	0	0	12
85.806	3	2	5	89.517	2	1	9	93.338	5	0	-2	97.330	1	-6	7
85.860	3	-1	8	89.646	4	-1	6	93.575	5	-4	-2	97.363	0	3	10
85.894	3	-5	-5	89.652	2	4	4	93.588	1	-4	10	97.533	1	6	0
86.123	2	-5	7	89.655	2	4	-7	93.638	0	4	-10	97.724	3	4	-5
86.129	2	-6	4	89.716	5	-3	1	93.697	2	-6	6	97.988	5	-4	-4
86.290	1	-3	10	89.719	4	2	-4	93.745	3	4	-3	98.138	5	-2	-6
86.354	3	-6	0	89.925	2	2	8	93.841	3	-5	7	98.222	5	-2	4
86.363	3	-6	1	89.962	2	3	-9	93.858	2	3	7	98.276	3	0	9
86.501	4	1	3	89.974	5	-1	-3	93.986	1	-5	-7	98.322	5	-4	3
86.650	4	0	-7	90.228	2	-4	9	94.132	1	4	7	98.455	0	2	-12
86.681	0	6	-2	90.344	4	-1	-8	94.146	3	2	-9	98.485	2	-4	10
86.768	2	-5	-6	90.502	5	-3	-3	94.175	5	0	0	98.513	2	2	9
86.885	2	3	6	90.525	4	-4	-6	94.217	2	-3	-10	98.627	5	0	2
86.954	0	0	11	90.658	1	2	-11	94.245	3	-2	-10	98.635	1	4	-10
87.144	2	-2	-10	90.953	5	-2	-4	94.499	4	0	6	98.753	1	6	-4
87.217	1	4	6	91.003	5	-2	2	94.534	1	-2	-11	98.932	4	0	-9
87.260	4	2	-2	91.006	2	0	-11	95.042	2	4	-8	99.041	2	-2	11
87.270	3	-6	2	91.165	1	4	-9	95.111	3	1	-10	99.409	4	-6	3
87.300	4	1	-6	91.304	1	-2	11	95.280	3	4	-4	99.420	4	-4	7
87.392	1	-5	-6	91.398	4	-2	-8	95.297	3	-6	-4	99.477	0	6	4
87.399	5	-2	0	91.493	3	-1	-10	95.331	4	-3	7	99.583	3	4	2
87.454	1	-4	-8	91.588	4	-5	4	95.334	2	5	1	99.798	3	-4	9
87.589	2	-4	-8	91.597	0	6	2	95.370	1	2	10	99.948	4	3	-1
87.705	0	2	10	91.754	2	-6	-4	95.496	4	-3	-8				
87.718	3	2	-8	91.772	3	-6	4	95.514	2	-4	-9				
87.774	3	3	-6	91.781	3	0	-10	95.564	5	-4	2				
87.833	4	-2	6	91.851	1	5	4	95.773	4	2	-6				
87.951	1	5	-6	92.003	5	-1	-4	95.872	4	-6	0				
88.151	4	-4	5	92.208	2	-1	-11	95.945	5	0	1				
88.244	3	-5	6	92.306	1	0	11	96.128	0	6	-6				

## § 2. Size distribution.

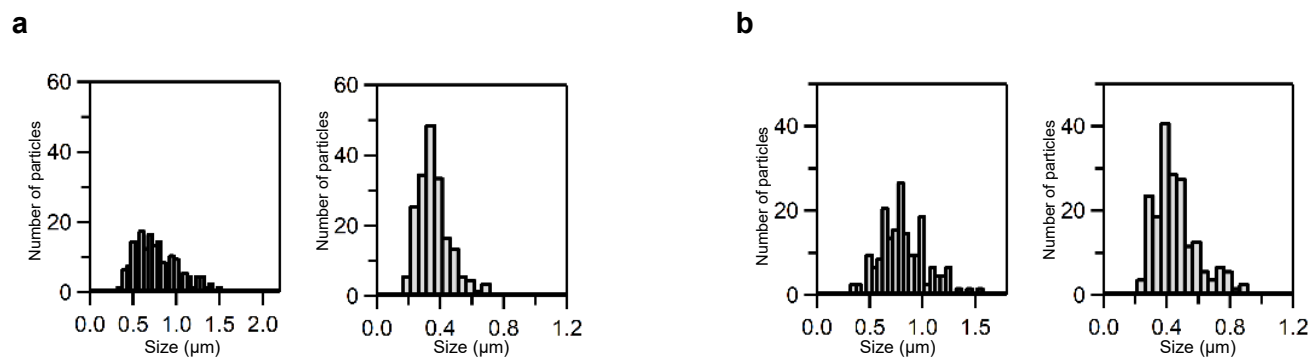


**Fig. S1.** Size distributions of (a) **1** and (b) **2** along the major (left) and minor (right) axes estimated from the SEM images.

### § 3. TEM images.

The TEM images of samples **1** and **2** (Figure S2) exhibit structures comprising sintered crystallites several tens of nanometers in size; the crystallites in **2** are larger than those in **1**.

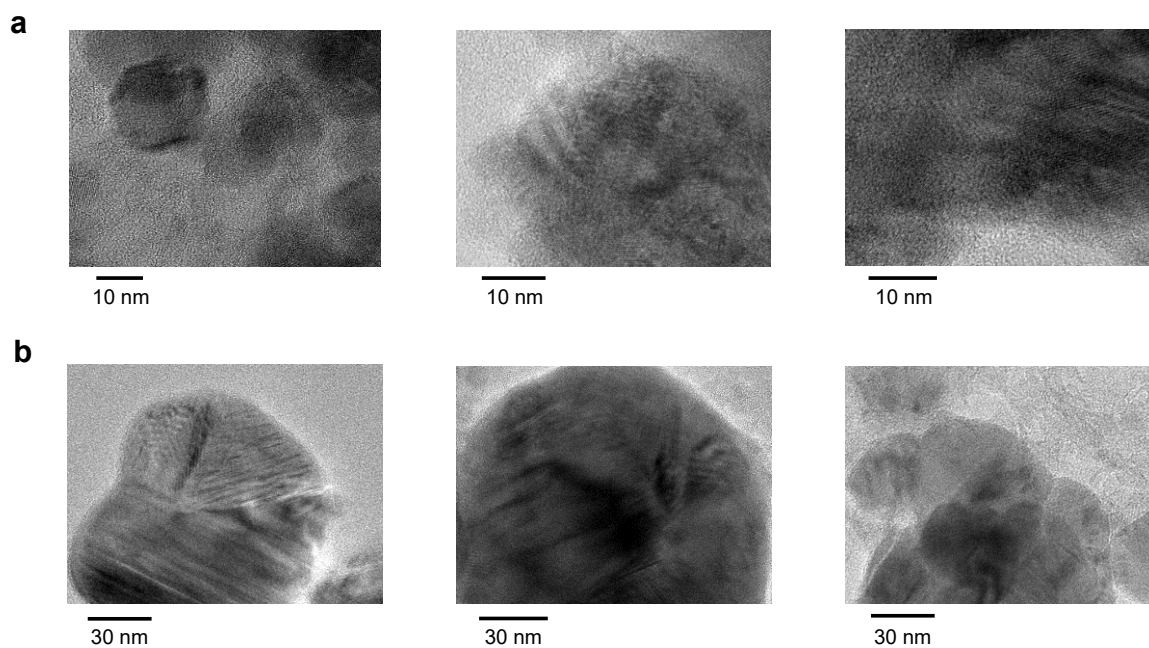


**Fig. S2.** TEM images of (a) **1** and (b) **2**.

#### § 4. XPS spectra at room temperature.

XPS measurements were conducted at room temperature using a JPS 9010 TR instrument (JEOL, Japan), equipped with an ultrahigh-vacuum chamber and an Al K $\alpha$  X-ray source (1486.6 eV). The pass energy was set at 10 eV, and the energy resolution, estimated from the width of the Ag 3d5/2 peak obtained for a clean Ag sample, was 0.635 eV. The uncertainty in the binding was  $\pm 0.05$  eV. A bulk Ti<sub>4</sub>O<sub>7</sub> crystal (OS-10A, Canon Optron) was used as the reference material. The samples were mounted on the holder using graphite tape. The Shirley background was subtracted from the spectrum using SpecSurf software (version 1.9.6.3; JEOL, Japan). The charge buildup in the graphite tape induced higher binding energy shifts for the spectra. To correct this, the charge-up amount was calibrated by setting the C 1s peak of the graphite tape at 284.6 eV in the spectrum of the reference sample. Based on this calibration, the energy scales were corrected by  $-1.749$ ,  $-1.510$ , and  $-1.485$  eV for **1**, **2**, and the reference sample, respectively.

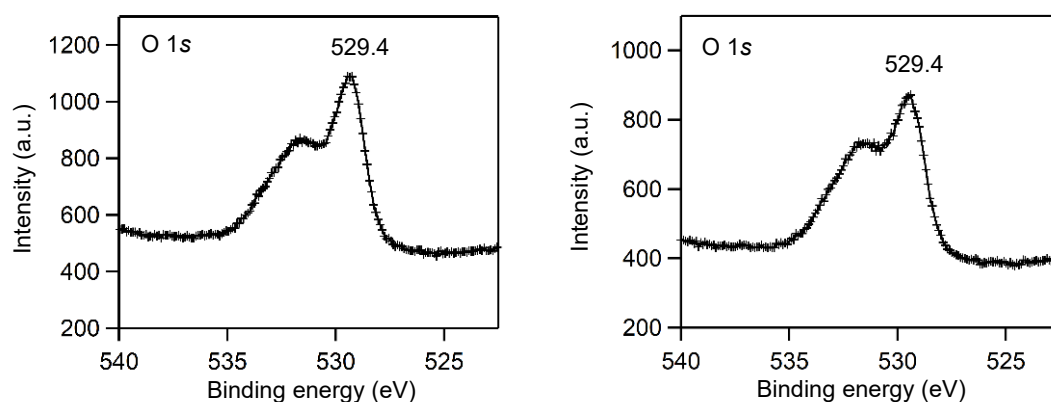


**Fig. S3.** O 1s XPS spectra of the synthesized sample **1** (left) and sample **2** (right).

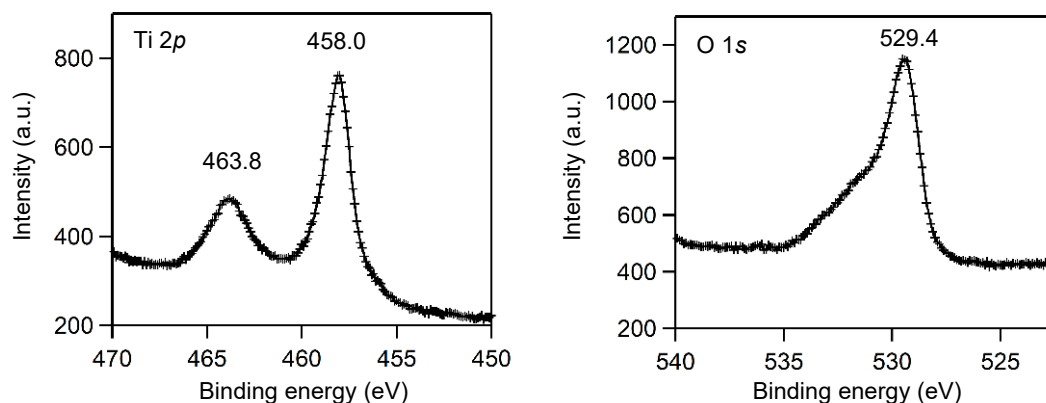


**Fig. S4.** XPS spectra of the bulk crystal reference sample: Ti 2p (left) and O 1s (right) XPS peaks.

## § 5. THz conductivity spectrum.

Figure S6 presents the results of terahertz time-domain spectroscopy (THz-TDS) of **1**, to evaluate its conductivity at room temperature. Owing to the metallic nature of the sample, which results in strong terahertz absorption, THz-TDS was performed in a reflection configuration. For THz-TDS measurement, the powder was pressed into a pellet. The complex conductivity,  $\tilde{\sigma} = \sigma' + i\sigma''$ , of the powder was derived from the effective conductivity of the pellet using the Bruggeman effective medium approximation, assuming spherical nanoparticles.<sup>[S1]</sup> The resulting THz conductivity spectra exhibit a positive slope in  $\sigma'$  and negative values of  $\sigma''$ , deviating from the conventional Drude response. This behavior is attributed to carrier localization within the nanoparticles, suppressing long-range electron transport.<sup>[S2,S3]</sup> To extract the direct-current (DC) or zero-frequency conductivity of the nanoparticles, the complex conductivity spectra were fitted using the Drude–Smith model, which incorporates localization effects in nanostructured materials:<sup>[S1–S4]</sup>

$$\tilde{\sigma} = \frac{\sigma_0}{1-i\omega\tau_{\text{DS}}} \left[ 1 + \frac{c}{1-i\omega\tau_{\text{DS}}} \right].$$

Here,  $\sigma_0$  is the DC conductivity,  $\omega$  is angular frequency,  $\tau_{\text{DS}}$  is the Drude–Smith scattering time, and  $c$  is the “localization parameter”, ranging from  $c = 0$  (free Drude behavior) to  $c = -1$  (complete carrier backscattering from interfaces or surfaces). The best-fit parameters obtained from the fitting are  $\sigma_0 = (719 \pm 15)$  S/cm,  $\tau_{\text{DS}} = (45 \pm 1)$  fs, and  $c = -0.971 \pm 0.001$ . These results suggest that the nanoparticles exhibit high conductivity, which is significantly suppressed by strong carrier localization. For comparison, the DC conductivity of single-crystal  $\text{Ti}_4\text{O}_7$  has been reported to be  $>1000$  S/cm.<sup>[S5]</sup> The reduced DC conductivity observed in the nanoparticles can be attributed to size effects.

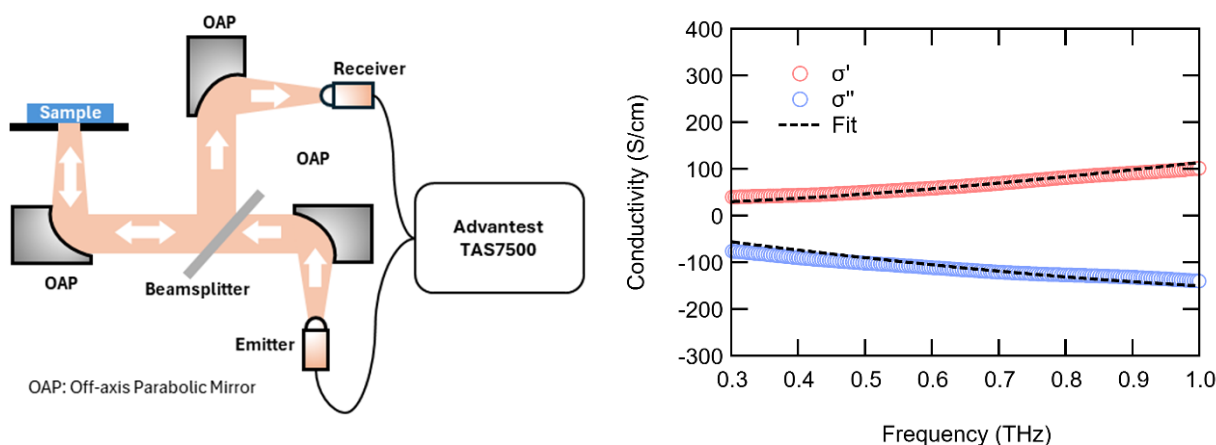


**Fig. S5.** Schematic illustration of the experimental setup for reflection THz-TDS measurements (left) and **1** (right) conductivity spectrum. The frequency resolution for THz conductivity measurements is 3.8 GHz.

[S1] J. B. Baxter and C. A. Schmuttenmaer, *J. Phys. Chem. B*, 2006, **110**, 25229.

[S2] N. V. Smith, *Phys. Rev. B*, 2021, **64**, 155106.

[S3] J. L. –Hughes and T. I. Jeon, *J. Infrared Millim. Te.*, 2012, **33**, 871.

[S4] G. M. Turner, M. C. Beard, and C. A. Schmuttenmaer, *J. Phys. Chem. B*, 2002, **106**, 11716.

[S5] R. F. Bartholomew and D. R. Frankl, *Phys. Rev.*, 1969, **187**, 828.

## § 6. Temperature dependence of Gibbs free energy.

To explain the relative stability of the two phases, we use the simple thermodynamic expression:

$$G_i = H_i - TS_i \quad (i = \text{LT, HT}) \quad \dots \quad (1)$$

where  $H$  is the enthalpy,  $T$  is the temperature,  $S$  is the entropy, and  $i$  denotes the phase, viz., the low-temperature (LT) phase (semiconductor phase) and the high-temperature (HT) phase (metallic phase). The difference in Gibbs free energy between the LT and HT phases ( $\Delta G$ ) can then be written as:

$$\Delta G = G_{\text{HT}} - G_{\text{LT}} = (H_{\text{HT}} - H_{\text{LT}}) - (TS_{\text{HT}} - TS_{\text{LT}}) = \Delta H - T\Delta S \quad \dots \quad (2)$$

At the phase transition temperature,  $\Delta G = 0$ . For  $\Delta G < 0$ , the HT phase has a lower free energy, and is therefore the thermodynamically stable phase, whereas for  $\Delta G > 0$ , the LT phase becomes the stable phase. Using the parameters used in the SD-model calculations in the main text,  $\Delta H = 500 \text{ J mol}^{-1}$  and  $\Delta S = 3.36 \text{ J K}^{-1} \text{ mol}^{-1}$  for sample **1**, the temperature dependence of  $\Delta G$  calculated from Eq. (2) is shown in Fig. S6a. Similarly, the results obtained for sample **2** using  $\Delta H = 850 \text{ J mol}^{-1}$  and  $\Delta S = 5.67 \text{ J K}^{-1} \text{ mol}^{-1}$  are presented in Fig. S6b. The phase transition temperatures ( $T_C$ ) were 149 K for **1** and 150 K for **2**. Below  $T_C$ ,  $\Delta G > 0$ ; therefore, the LT phase (semiconductor phase) is thermodynamically stable. In contrast, above  $T_C$ ,  $\Delta G < 0$ ; therefore, the HT phase (metallic phase) becomes stable.

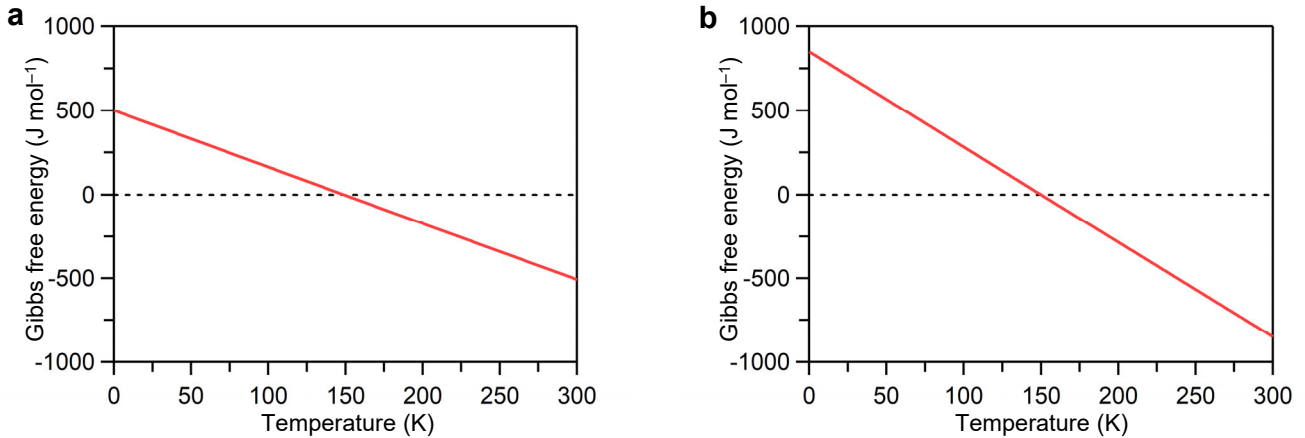


**Fig. S6.** Temperature dependence of Gibbs free energy. Calculated with (a)  $\Delta H = 4.3 \text{ kJ mol}^{-1}$  and  $\Delta S = 29.8 \text{ J K}^{-1} \text{ mol}^{-1}$  for **1** and (b)  $\Delta H = 4.3 \text{ kJ mol}^{-1}$  and  $\Delta S = 29.8 \text{ J K}^{-1} \text{ mol}^{-1}$  for **2**.

## § 7. Gaussian distribution of crystallite size.

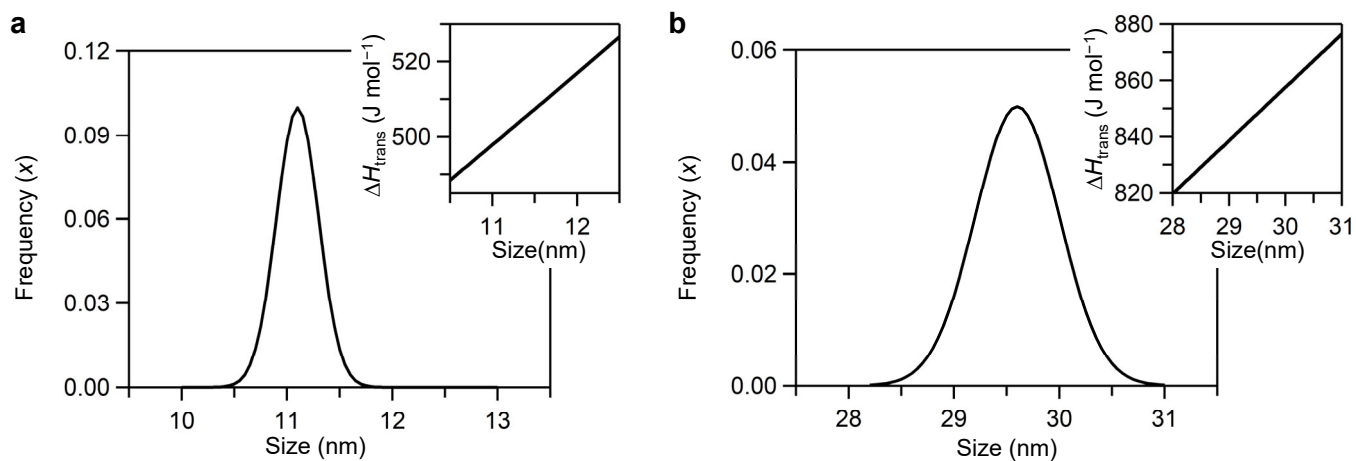


**Fig. S7.** Gaussian distribution of crystallite sizes for (a) **1** and (b) **2**. Based on the results of Rietveld refinement, the average particle size of **1** was 11.1 nm with a standard deviation of 0.2 nm, and the corresponding values for **2** were 29.6 nm and 0.4 nm. The inset graphs (upper right) show the relationship between crystallite size and  $\Delta H_{\text{trans}}$ , indicating the  $\Delta H_{\text{trans}}$  values used in the SD model calculations for each size.

## § 8. Relationship between Gibbs free energy, crystallite size, and transition enthalpy.

For nanocrystallites, the Gibbs free energy ( $G = H - TS$ , where  $H$  is enthalpy,  $T$  is temperature,  $S$  is entropy), including the contribution of surface (interfacial) energy can be described as follows:

$$G = G_B + (6V_m/d)G_S.$$

Here,  $G_B$  is the bulk free energy,  $G_S$  is the surface (or interfacial) free energy,  $V_m$  is the molar volume, and  $d$  is the diameter of the nanocrystallite. The free energy difference ( $\Delta G$ ) between the low-temperature (LT) and high-temperature (HT) phases is expressed as follows:

$$\Delta G = G_{HT} - G_{LT} = [G_{B,HT} - G_{B,LT}] + [(6V_{m,HT}/d)G_{S,HT} - (6V_{m,LT}/d)G_{S,LT}].$$

For intuitive understanding, we consider the case at absolute zero temperature. Because the Gibbs free energy of the LT phase is lower than that of the HT phase, the relation  $G_{B,HT} > G_{B,LT}$  holds, and thus  $[G_{B,HT} - G_{B,LT}]$  takes a positive value. On the other hand, the LT phase generally has a higher density, and consequently, a higher surface (interfacial) free energy than the HT phase, i.e.,  $G_{S,HT} < G_{S,LT}$  is expected. Therefore, depending on the value of  $V_m$ , the term  $[(6V_{m,HT}/d)G_{S,HT} - (6V_{m,LT}/d)G_{S,LT}]$  generally takes a negative value, and its magnitude becomes more negative as crystallite size  $d$  decreases. In a system where the relationship between the positive contribution  $[G_{B,HT} - G_{B,LT}]$  and the negative contribution  $[(6V_{m,HT}/d)G_{S,HT} - (6V_{m,LT}/d)G_{S,LT}]$  causes  $\Delta G$  to decrease with decreasing crystallite size  $d$ , the transition enthalpy ( $\Delta H$ ) also decreases with decreasing value of  $d$ . Such effects have been observed in  $\text{Al}_2\text{O}_3$ ,<sup>S6</sup>  $\text{Fe}_2\text{O}_3$ ,<sup>S7</sup> and  $\text{Ti}_3\text{O}_5$ .<sup>S8</sup> In particular, for  $\text{Ti}_3\text{O}_5$ , the  $\Delta H$  reportedly varies almost linearly with crystallite size.<sup>S9</sup>

[S6] J. M. McHale, A. Auroux, A. J. Perrotta, and A. Navrotsky, *Science*, 1997, 277, 788–791.

[S7] S. Ohkoshi, S. Sakurai, J. Jin, and K. Hashimoto, *J. Appl. Phys.*, 2005, 97, 10K312.

[S8] S. Ohkoshi, Y. Tsunobuchi, T. Matsuda, K. Hashimoto, A. Namai, F. Hakoe, and H. Tokoro, *Nat. Chem.*, 2010, 2, 539–545.

[S9] T. Kubota, R. Seiki, A. Fujisawa, A. F. Fadilla, F. Jia, S. Ohkoshi and H. Tokoro, *Mater. Adv.*, 2024, 5, 3832–3837.